Fugacity Coefficients of Saturated Water from Molecular Simulation

Scott J. Wierzchowski and David A. Kofke*

Department of Chemical Engineering, University at Buffalo, The State University of New York, Buffalo, New York 14260-4200

Received: April 25, 2003; In Final Form: July 17, 2003

We apply isothermal−isobaric Monte Carlo molecular simulation to measure the vapor-phase fugacity coefficients and equation of state of three fixed-charge models of water: SPC/E, MSPC/E, and TIP3P. State conditions correspond to the experimental vapor−liquid saturation pressures for temperatures between 292.65 and 386.85 K. The results are compared to the experimental data for water vapor. We also examine properties as given by the application of the virial equation of state, using values of the second virial coefficients computed by us or that have been previously reported (in some cases up to third virial coefficients) for the models simulated here. The models show significant deviation from ideal-gas behavior, considerably more than seen experimentally, and a second-order virial treatment does not fully characterize the behavior. This deviation from experiment is consistent with the expected failings of fixed-charge models developed for liquid phases, when applied to the vapor. A virial-equation treatment of a fluctuating-charge model (TIP4P/fq) and the polarizable point charge model (PPC) indicates that the vapor-phase properties of these models will be much more in line with experimental fugacities and densities along the coexistence line.

Introduction

The immense quantity of scientific studies involving water is motivated by the nearly ubiquitous presence of water in natural and man-made processes. Despite decades of study, there is still much room for improvement in our ability to model and understand the molecular origins of the behavior of water.[1,2] For example, a famous peculiarity of water is the density peak in the liquid phase near freezing, yet the scope of the microscopic behavior that accompanies this feature is still being uncovered.[3−6]

The need to predict and understand water properties, particularly as a solvent and in mixtures, has stimulated work toward its quantitative molecular modeling. To this end, it is important first to describe pure water well, and to do so over a wide range of conditions. This latter issue is paid less attention, but it is important to the formulation of a robust model, one that appropriately captures the influence of water on solutes even if just at ambient conditions. The goal of understanding water via molecular models has attracted countless researchers' efforts.[7−10] Along the way a wide variety of pure-fluid properties have been calculated through application of some notable potential models. Significant effort has been given to detailing radial distribution functions by molecular simulation[11] and reconciling them with corresponding experimental measurements.[12] Likewise, vapor−liquid equilibrium,[13−16] diffusion coefficients,[17] surface tension,[18] and many other properties have been subjects of study using established water models.

Efforts to develop molecular models for water range from ab initio derived potential models[19,20] to empirically fit models. Many models couple Lennard-Jones terms with point charges to define the water molecule.[21−26] A more recent trend is incorporation of multi-body effects through fluctuating charges and polarization treatments.[7,15,27,28] Other efforts have tried to incorporate quantum mechanical (QM) energies to predict water properties.[29−31] The computational expense of QM methods discourages their routine use, and most modeling applications employ van der Waals forces with point-charge electrostatics, perhaps with polarization.

The vapor phase of water draws much less modeling attention than the liquid. One reason is just that the liquid is practically more important than the vapor. Nevertheless, the vapor is not inconsequential. Rather, it may be that hydrogen bonding or association of vapor water molecules is less pronounced than in liquid water, and there is less challenge in the modeling. Likewise, the experimentally measured fugacity coefficients and equation of state of the saturated vapor are close to ideal, and consequently, the ideal-gas law or perhaps the virial equation of state can provide an adequate description of the behavior. Still, molecular models of water are applied to the vapor phase, often because of interest in its connection to the liquid, such as in calculations of vapor−liquid-phase coexistence properties or interfacial tension. If the vapor is in fact well modeled as an ideal gas, we wish for the molecular model of it to maintain this feature. If the model has too-strong interactions (in comparison to real water), it might exhibit inappropriate deviations from ideal-gas behavior. A frame of mind that sees the vapor as ideal might well overlook this effect when trying to reconcile deviations of the model from experiment in, for example, vapor−liquid coexistence behavior. In fact in many cases, the vapor model does show nonidealities where the real vapor does not, and in this work, we aim to highlight this point. We emphasize the behavior of the chemical potential, expressed via the fugacity coefficient, because this property connects most directly to factors involving equilibria with the liquid and other phases.

In the following, we examine several three-charge potential models for water. We use isothermal−isobaric Monte Carlo simulations to calculate fugacity coefficients and compressibility factors for saturated water vapor. The calculated data are compared to the experiment to determine how effective the

* To whom correspondence should be addressed.

10.1021/jp0351270 CCC: $25.00
Published on Web 10/25/2003

TABLE 1: Parameters for the Potential Models Used[a]

H_2O model	σ(Å)	ϵ(kcal/mol)	q(e)	a_{HOH} (°)	r_{OH} (Å)	μ(D)
TIP3P	3.151	0.152	0.4170	104.95	0.9572	2.348
SPC/E	3.166	0.155	0.4238	109.47	1.0000	2.35
MSPC/E	3.116	0.148	0.4108	109.47	0.9839	2.24
expt.				104.45	0.958	1.85

[a] Each potential model consists of a Lennard-Jones van der Waals term and three point charges (eq 1). A charge of $-2q$ is located on the oxygen atom. Two charges of $+q$ for hydrogen atoms are placed a distance of r_{OH} from the oxygen making an angle of a_{HOH}; μ is the dipole moment in Debye. Experimental values for the geometry and dipole moment are for the gas-phase water molecule.[44]

methodologies and potential models are for the saturated water vapor conditions. We also use literature and our own values for virial coefficients of the models to calculate the same properties and establish the range of validity of the virial equation. We examine the same properties for polarizable water models using virial coefficients known for them. In section II, we describe the potentials and methods. We briefly describe the simulation details in section III. In section IV, we present the calculated fugacity coefficients and compressibility factors. Finally, section V makes conclusions.

Methodology

Potential Models. Simulations performed in this study examine several nonpolarizable three-site models for water. In particular, we examine the TIP3P,[23] SPC/E,[24] and MSPC/E[26] model. Each model is described by two Lennard-Jones parameters, σ and ϵ, for oxygen-atom interactions, an OH bond length, r_{OH}, an HOH bond angle, a_{HOH}, and three charges, q, $-2q$, and q. In Table 1, the parameters are collected. MSPC/E is exactly related to SPC/E via corresponding states, but because we study along only a single pressure−temperature line, the models provide independent data. The energy is calculated according to

$$U_{ij} = 4\epsilon\left(\left(\frac{\sigma}{r_{oo}}\right)^{12} - \left(\frac{\sigma}{r_{oo}}\right)^{6}\right) + \sum_{a=1}^{3}\sum_{b=1}^{3}\frac{q_i^a q_j^b e^2}{r_{ij}^{ab}} \qquad (1)$$

In addition, Ewald summation was implemented for the calculation of long-range electrostatic interactions. The details of the application of the Ewald technique can be found elsewhere.[32]

We examine two polarizable models, but only through their published virial coefficients—no simulations are conducted for them. The models are TIP4P/fq and polarizable point charge model (PPC).[27,33]

Fugacity and the Widom Method. The particle insertion method or Widom method[34] involves the repeated random insertion of a molecule into the simulated phase, without affecting the configurations sampled by the other molecules, and thereby yields the chemical potential as an appropriate ensemble average.[35] In the NPT ensemble, the working equation is

$$\mu = -kT\ln(kTq/P\Lambda^3) - kT\ln\left[\frac{P}{(N+1)kT}\langle V\exp(-\beta\Delta U)\rangle\right] \qquad (2)$$

where P is the pressure, N is the number of molecules, T is the temperature, k is Boltzmann's constant, V is the instantaneous volume, Λ is the de Broglie wavelength, q represents the rest of the single-molecule partition function, $\beta = 1/kT$, and ΔU is the change in energy upon insertion of the test molecule. The last term on the right-hand side of this equation gives the fugacity coefficient ϕ

$$\phi = \frac{(N+1)kT}{P\langle V\exp(-\beta\Delta U)\rangle} \qquad (3)$$

which is the quantity we use to report our results for the chemical potential.

Fugacity and the Tripathi−Chapman Method. The insertion method is known to be problematic in application to dense phases,[36] because significant contributions to the average are made by the relatively few configurations in which the inserted molecule does not overlap one of the simulated molecules. This is not an issue for the gas-phase systems we are studying, but instead, a similar problem arises. In strongly associating systems, such as water that forms hydrogen bonds, significant contributions come from insertion of the test molecule into the hydrogen-bonding region of another molecule. This too may be a rare occurrence, and a straightforward application of the Widom method might lead to inaccurate results. Tripathi and Chapman[37] recently introduced an insertion methodology to address this problem, and we apply their technique in our study.

The idea of the method is to define the "monomer" as a distinct species, and to use insertion to measure its chemical potential only. Standard thermodynamics states that the monomer chemical potential will equal the chemical potential of the species (taken without consideration of its state of aggregation), so measurement of the monomer chemical potential gives directly the species chemical potential of interest. The insertion average gives only the chemical potential above the ideal-gas value, so to get the full chemical potential, we need also to measure the "mole fraction" of the monomer in the system. This is easily taken as part of the ensemble average. With this view, the working equation for the chemical-potential measurement becomes

$$\mu = -kT\ln(kTq/P\Lambda^3) - kT\ln\left[\frac{P}{kT}\left\langle\frac{V}{N_{mono}+1}\exp(-\beta\Delta U_{mono})\right\rangle\right] \qquad (4)$$

where N_{mono} is the instantaneous number of monomers in the system, and ΔU_{mono} is the energy of the inserted molecule, which contributes to the ensemble average only if its random insertion finds it to be a monomer (otherwise the insertion attempt is discarded). The fugacity coefficient is

$$\phi = \left[\frac{P}{kT}\left\langle\frac{V}{N_{mono}+1}\exp(-\beta\Delta U_{mono})\right\rangle\right]^{-1} \qquad (5)$$

Any definition of "monomer" can be applied when using this method. Logical choices would be based on an energetic (e.g., monomer if the energy of the molecule is within some tolerance of zero) or geometric (monomer if not in a particular hydrogen-bonding configuration) criterion. The usual Widom method is recovered if all molecules are taken to be "monomers" regardless of their situation.

UB Biasing Algorithm. In some sense, the Tripathi−Chapman algorithm pushes off the problem of insertion sampling into the problem of sampling configurations of the interacting molecules. Its validity is based on obtaining accurate values for the monomer number, N_{mono}. This measurement can also be a problem for associating systems, as its accurate characterization requires that molecules move between monomeric and nonmonomeric states with good frequency. Biasing

methods have been developed to address this problem,[38,39] and we apply one of them in our work.

The UB biasing algorithm has shown good performance in simulating low-density associating systems.[39,40] Previous applications have ranged from associating square-well models to hydrogen fluoride vapor phase. The methodology is based upon the definition of "Unbound" and "Bound" (UB) states described by a geometric region. Two Monte Carlo trial moves are used (in addition to the usual ones for NPT simulations of water), a *bonding* trial and an *unbonding* trial. Thus, attempts are made with equal frequency to move a molecule either explicitly into or out of a biasing region, defined here to coincide with the definition of whether a molecule is a monomer or not. The algorithm counts the number of *unbound* molecules before and after the transition, N_i^{mono} and N_j^{mono}. Similarly, the algorithm counts the number of biasing regions that the chosen molecule is in before and after the transition, n_i and n_j. The move is accepted with the probability of $\min(1,\chi)$, where

$$\chi = \frac{(N-1)\epsilon\delta_j + n_i(N - N_j^{\text{mono}})}{(N-1)\epsilon\delta_i + n_j(N - N_i^{\text{mono}})} \frac{(N - N_i^{\text{mono}})}{(N - N_j^{\text{mono}})} \exp(-\beta(U_j - U_i)) \quad (6a)$$

with

$$\delta_i,\delta_j = \begin{cases} 0 & \text{unbound in state } i, j \\ 1 & \text{bound in state } i, j \end{cases} \quad (6b)$$

and ϵ is the fraction of the "bound" volume to the volume of the phase. In principle the appearance of the product of ϵ with the Boltzmann factor of the energy change makes the value of χ close to unity, causing most trials to be accepted. Further details are presented in ref 39.

Virial Equation. The virial equation of state provides an alternative route to the thermodynamics of the vapor phase. It is appealing in the present circumstances because the coefficients appearing in the virial equation can be computed rigorously for a given intermolecular potential. The virial equation has a limited range of application, losing accuracy as the pressure is increased, and we use our simulation results to characterize its validity for the range of state conditions examined in this work.

The density-explicit form of the virial equation is appropriate to the present study because we work with pressure rather than density as an independent variable. In this formulation, the virial expression for the compressibility factor is

$$Z = \frac{PV}{RT} = 1 + B'P + C'P^2 + \ldots \quad (7a)$$

with the coefficients defined as

$$B' = \frac{B}{RT} \quad (7b)$$

$$C' = \frac{C - B^2}{(RT)^2} \quad (7c)$$

where the unprimed coefficients are the usual ones for the pressure-explicit expansion; R is the gas constant. If truncated at the order shown, the fugacity coefficient is

$$\ln \phi_{\text{sat}} = \int_0^{P_{\text{sat}}} \frac{Z-1}{P}\, dP = B'P_{\text{sat}} + \frac{1}{2}C'P_{\text{sat}}{}^2 \quad (8)$$

Second virial coefficients,[26,41−43] and in some cases third,[41] for the models studied here are available in the literature. However, they are reported for temperatures that incompletely overlap the states of interest here, so we have calculated the second-virial coefficients over the range of temperature of interest to this study. Figure 1 shows all second-virial coefficient values used here.

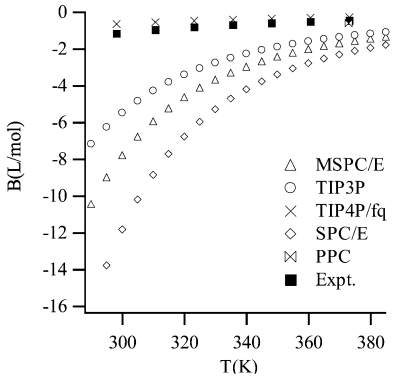

Figure 1. Second virial coefficients of water as calculated by us for MSPC/E, SPC/E, and TIP3P models, and from literature for TIP4P/fq,[16] PPC,[41] and experiment.[16,47]

TABLE 2: Saturated Water Vapor Conditions[45] Used for These Simulation[a]

P^{sat}(mmHg)	T(K)	Z	P^{sat}(mmHg)	T(K)	Z
17.0	292.65	0.999	301.4	349.15	0.991
17.3	292.95	0.997	801.6	374.65	0.984
17.9	293.45	1.000	1195.3	381.65	0.980
31.5	302.95	0.998	1215.2	386.55	0.980
43.4	308.65	0.998	1021.5	386.85	0.979
129.8	330.25	0.994			

[a] Z is the experimental value of the compressibility factor.[46]

Simulation Details. We performed NPT Monte Carlo simulations for several models of water: TIP3P,[23] SPC/E,[24] and MSPC/E.[26] The potential parameters defining these models are summarized in Table 1. State conditions followed the experimental values of the saturated vapor pressure for temperatures $T = 292.65-386.85$ K; conditions simulated are described in Table 2. Each simulation employed the UB bias algorithm, and measured the fugacity coefficient using the Tripathi-Chapman insertion algorithm discussed in section II as well as straightforward Widom insertion; the ensemble-averaged volume was also recorded.

Each simulation employed $N = 500$ water molecules. The percentage of each trial move was approximately 40% translation moves, 40% rotation moves, 20% UB biasing moves, with a fraction $1/N$ of volume moves. The simulations were relaxed for 2×10^4 cycles, where a cycle consists of N Monte Carlo trials; results were collected over 1×10^6 cycles.

For the Tripathi−Chapman and the UB algorithms respectively, a common geometry-based definition was used for describing a "monomer" and an "unbound" molecule. A molecule is considered a monomer, or unbound, if its oxygen atom lies more than 3.75 Å from any other oxygen atom.

Results and Discussion

Figures 2−4 display measured values of the fugacity coefficients for the MSPC/E, SPC/E, and TIP3P models, respectively. Figure 5 presents the compressibility factor for all of them. All data are for temperature/pressure combinations corresponding to the experimental vapor−liquid coexistence conditions. The true vapor pressures of some of these models are lower than the experimental values, and consequently, these

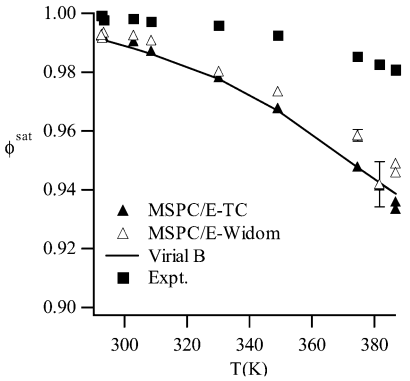

Figure 2. Fugacity coefficients as calculated from NPT simulations of the MSPC/E potential model. The pressure for each point is that of the experimental saturated vapor at the given temperature (Table 2). Closed triangles represent calculation from the Tripathi and Chapman (TC) method; open triangles are results from the Widom method. Error bars are indicated only when larger than the symbol size. Closed squares are the experimental data.[46] The line corresponds to the second-order virial equation using MSPC/E virial coefficients shown in Figure 1.

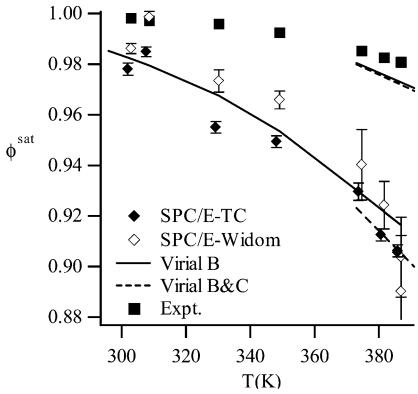

Figure 3. Same as Figure 2, but for the SPC/E potential model. Solid and hashed lines respectively correspond to second and third virial coefficient evaluation. Lines near the simulation data use virial coefficients for the SPC/E model; short lines at right and near experimental data use literature coefficients[41] for the PPC model.

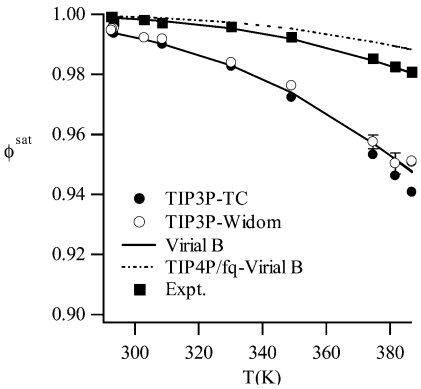

Figure 4. Same as Figure 2, but for the TIP3P potential model. Also shown are data for the TIP4P/fq model based on the second virial coefficient.[16] Solid lines through simulation and experimental data are based on the second-virial coefficient for the TIP3P model (Figure 1) and experiment,[16,47] respectively.

models are studied at metastable conditions; we do not expect this fact to adversely affect our analysis, as long as the vapor does not condense. Also presented on each plot are experimental data, as well as curves representing application of the virial equation.

There are two points to consider in examining these results. First, we are interested in the ability of each potential model to reproduce the behavior of the vapor at the experimental saturation conditions; if the models do not, this information goes some way toward understanding why the models disagree with experimental vapor pressures. Second, it is also of interest to consider effectiveness of the simulation methodology to measure fugacity coefficients. The data are displayed in a manner so the methodology can be compared for each separate model. The ability of the potential model to represent saturated water vapor can be derived from a comparison with the experimental results, which are common to Figures 2−4.

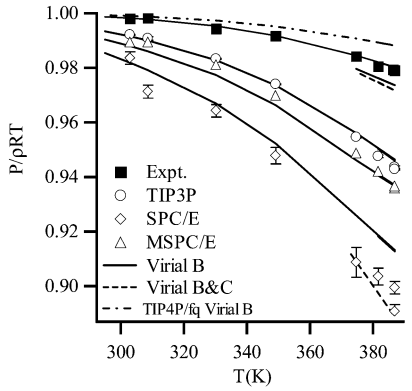

Figure 5. Compressibility factor for saturated water vapor for the potential models studied here, compared with experiment.[46] Solid and hashed lines respectively describe results from the second and third (for PPC and SPC/E models) virial coefficient evaluation, with solid lines corresponding to data points nearest to each line. Also shown are second-virial results for TIP4P/fq model.

Considering first the performance of the methods, the Tripathi−Chapman results show consistently greater precision than direct Widom insertion, as indicated by their smaller error bars. There is also a small but consistent difference between the results. The Tripathi−Chapman data are consistently below the Widom data. This observation is consistent with our understanding of the manner of failure of the Widom method for associating systems. Insufficient sampling of the energetically favorable configurations causes the basic Widom insertion method to underestimate the ensemble average, and thereby overestimate the fugacity coefficient. Comparison with the virial equation also tends to support the conclusion that the Tripathi−Chapman based data are of greater accuracy.

The main statement to be made regarding the behavior of the measured fugacity coefficients is that the molecular models significantly underestimate the experimental values. This result is consistent with the corresponding data for the compressibility factor, which shows that the models overestimate the experimental density at each condition. In all cases, the molecular models indicate greater deviation from ideal behavior than observed in the experimental data. This trend is easily understood and has been explained by others:[16] the molecular models examined here have been developed to describe liquid-phase properties, and consequently, they possess dipole moments that are significantly greater than the gas-phase value. This leads them to interact more strongly than is appropriate, with greater association, resulting in larger and more negative deviations from ideal-gas behavior. The trend in the models' dipole moments is SPC/E $\approx$ TIP3P > MSPC/E. Correspondingly, SPC/E displays the largest deviation from experiment, but MSPC/E and TIP3P are both somewhat better, with results about equal to each other (albeit still poor in comparison with experiment). Thus, the dipole moment is not the sole determinant of the degree of nonideality. Noting that the dipole moment is more physically useful when considering interactions that are

more distant, perhaps slightly more important in this context is the O−H bond length r_{OH} itself (cf. Table 1): SPC/E > MSPC/E > TIP3P. So TIP3P does better than SPC/E despite the comparable dipole because the smaller OH bond prevents the electrostatic energy for closely separated molecules from becoming as negative (which would contribute to a more nonideal, SPC/E-like fugacity coefficient). Still, the dipole moment is not irrelevant, as TIP3P has the correct gas-phase geometry, but displays poor agreement due to the exaggerated charges needed to describe the liquid. The features contributing to the poor performance of the SPC/E model also contribute to difficulties in simulating it in the vapor. Results for it are significantly more scattered than for the other systems, and the discrepancy between the scatter and the confidence limits indicates problems in converging the NPT simulation volume.

Comparison with the curves obtained via the virial equation indicate the limitations of the virial equation in describing the vapor phase. The vapor becomes increasingly nonideal at higher temperatures, where the pressure is greater. In all cases, the comparison shows that the second-order virial equation (i.e., including B only) does not fully describe the deviation from ideality. For the SPC/E model, where we do have data for the third virial coefficient, we find that this additional correction is sufficient to bring the virial model in line with the simulation data.

The failure of fixed-charge models (such as the ones studied here) to capture vapor and liquid-phase behavior has motivated the development of polarizable and fluctuating-charge models. Such models adapt to their environment, so that they exhibit liquidlike charge distributions when in the liquid, while recovering the appropriate gas-phase dipole moment when in the gas. We have not performed corresponding simulations for such models, but instead, we examine their behavior in terms of their known virial coefficients. Our comparison of the virial formula with simulation data for the nonpolarizable models gives a good indication of the appropriateness of the virial equation for this purpose. Figure 4 includes the fugacity coefficient for the TIP4P/fq fluctuating-charge model as given by the second-order virial equation, whereas Figure 5 shows the same for the compressibility factor. Figure 3 includes the fugacity coefficient for the PPC model as given by the second- and third-order virial equations, whereas Figure 5 again shows the same for the compressibility factor. The improvement is clear and gives a strong indication of the value of using polarizable models when studying the vapor phase in conjunction with a liquid.

Conclusion

This work highlights issues involved in molecular modeling as applied to the description of the vapor phase. These considerations can be useful in guiding the formulation of comprehensive molecular models capable of describing both liquid and vapor phases. The more thoroughly characterized molecular models have been examined for their vapor−liquid coexistence properties.[3,15,16,26] The vapor pressure is commonly viewed as a liquid-phase property, in that its value is almost fully established by the chemical potential of the liquid phase. This view assumes that the vapor is ideal. Such an assumption may be well justified, at least from the standpoint of the behavior of the physical system being modeled. In this work, we emphasize the point that, although the actual vapor might be reasonably described as ideal, molecular models for it will tend to fail in a way that cause it to deviate more from ideal behavior. In this case, attempts to improve vapor−liquid coexistence properties by focusing on the liquid phase will be at least partially misdirected. In this regard, it is notable that the MSPC/E model was optimized to match experimental vapor pressures; that it does this while giving a less-than-adequate description of the vapor indicates that it has only achieved a cancellation of errors between the vapor and liquid.

We find that all fixed-charge models for water exhibit a much more nonideal vapor phase then is seen experimentally. Indications are that the use of a fluctuating-charge model remedies this error considerably. The Tripathi−Chapman method provides a good means to measure chemical potentials of associating systems, particularly when used in conjunction with an association-bias sampling algorithm.

Acknowledgment. Financial support was provided by the National Science Foundation, Grant CTS-0076515. Computing facilities were provided by the University at Buffalo Center for Computational Research. We thank Jeffrey Errington for a critical reading of the manuscript.

References and Notes

(1) Finney, J. L. *J. Mol. Liq.* **2001**, *90*, 303.
(2) Nezbeda, I.; Weingerl, U. *Mol. Phys.* **2001**, *99*, 1595.
(3) Lisal, M.; Kolafa, J.; Nezbeda, I. *J. Chem. Phys.* **2002**, *117*, 8892.
(4) Mahoney, M. W.; Jorgensen, W. L. *J. Chem. Phys.* **2000**, *112*, 8910.
(5) Truskett, T. M.; Debenedetti, P. G.; Sastry, S.; Torquato, S. *J. Chem. Phys.* **1999**, *111*, 2647.
(6) Errington, J. R.; Debenedetti, P. G. *Nature* **2001**, *409*, 318.
(7) Stern, H. A.; Kaminski, G. A.; Banks, J. L.; Zhou, R. H.; Berne, B. J.; Friesner, R. A. *J. Phys. Chem. B* **1999**, *103*, 4730.
(8) Chialvo, A. A.; Cummings, P. T. *J. Chem. Phys.* **1996**, *105*, 8274.
(9) Nezbeda, I. *J. Mol. Liq.* **1997**, *73*−*4*, 317.
(10) Chialvo, A. A.; Cummings, P. T. *Adv. Chem. Phys.* **1999**, *109*, 115.
(11) Chialvo, A. A.; Cummings, P. T. *J. Phys. Chem.* **1996**, *100*, 1309.
(12) Soper, A. K.; Bruni, F.; Ricci, M. A. *J. Chem. Phys.* **1997**, *106*, 247.
(13) Liew, C. C.; Inomata, H.; Arai, K. *Fluid Phase Equilib.* **1998**, *144*, 287.
(14) Mackie, A. D.; Hernandez-Cobos, J.; Vega, L. F. *Mol. Simul.* **2000**, *24*, 63.
(15) Rivera, J. L.; Predota, M.; Chialvo, A. A.; Cummings, P. T. *Chem. Phys. Lett.* **2002**, *357*, 189.
(16) Medeiros, M.; Costas, M. E. *J. Chem. Phys.* **1997**, *107*, 2012.
(17) Mahoney, M. W.; Jorgensen, W. L. *J. Chem. Phys.* **2001**, *114*, 363.
(18) Alejandre, J.; Tildesley, D. J.; Chapela, G. A. *J. Chem. Phys.* **1995**, *102*, 4574.
(19) Clementi, E.; Corongiu, G. *Int. J. Quantum Chem.* **1983**, 31.
(20) Mas, E. M.; Bukowski, R.; Szalewicz, K.; Groenenboom, G. C.; Wormer, P. E. S.; van der Avoird, A. *J. Chem. Phys.* **2000**, *113*, 6687.
(21) Stillinger, F. H.; Rahman, A. *J. Chem. Phys.* **1974**, *60*, 1545.
(22) Jorgensen, W. L. *J. Chem. Phys.* **1982**, *77*, 4156.
(23) Jorgensen, W. L.; Chandrasekhar, J.; Madura, J. D.; Impey, R. W.; Klein, M. L. *J. Chem. Phys.* **1983**, *79*, 926.
(24) Berendsen, H. J. C.; Grigera, J. R.; Straatsma, T. P. *J. Phys. Chem.* **1987**, *91*, 6269.
(25) Jorgensen, W. L.; Chandrasekhar, J.; Madura, J. D.; Impey, R. W.; Klein, M. L. *J. Chem. Phys.* **1983**, *79*, 926.
(26) Boulougouris, G. C.; Economou, I. G.; Theodorou, D. N. *J. Phys. Chem. B* **1998**, *102*, 1029.
(27) Svishchev, I. M.; Kusalik, P. G.; Wang, J.; Boyd, R. J. *J. Chem. Phys.* **1996**, *105*, 4742.
(28) Martin, M. G.; Chen, B.; Siepmann, J. I. *J. Chem. Phys.* **1998**, *108*, 3383.
(29) Gao, J. *J. Chem. Phys.* **1998**, *109*, 2346.
(30) Honda, K. *J. Chem. Phys.* **2002**, *117*, 3558.
(31) Izvekov, S.; Voth, G. A. *J. Chem. Phys.* **2002**, *116*, 10372.
(32) Nymand, T. M.; Linse, P. *J. Chem. Phys.* **2000**, *112*, 6152.
(33) Kusalik, P. G.; Svishchev, I. M. *Science (Washington, D.C.)* **1994**, *265*, 1219.
(34) Widom, B. *J. Chem. Phys.* **1963**, *39*, 2808.
(35) Frenkel, D.; Smit, B. *Understanding Molecular Simulation: From Algorithms to Applications*; Academic Press: New York, 1996.
(36) Kofke, D. A.; Cummings, P. T. *Mol. Phys.* **1997**, *92*, 973.
(37) Tripathi, S.; Chapman, W. G. *Mol. Phys.* **2003**, *101*, 1199.

(38) Chen, B.; Siepmann, J. I. *J. Phys. Chem. B* **2000**, *104*, 8725.
(39) Wierzchowski, S.; Kofke, D. A. *J. Chem. Phys.* **2001**, *114*, 8752.
(40) Wierzchowski, S.; Kofke, D. A. *Fluid Phase Equilib.* **2002**, *194*, 249.
(41) Kusalik, P. G.; Liden, F.; Svishchev, I. M. *J. Chem. Phys.* **1995**, *103*, 10169.
(42) Kong, Y. C.; Nicholson, D.; Parsonage, N. G. *Mol. Simul.* **1994**, *13*, 39.
(43) Stern, H. A.; Rittner, F.; Berne, B. J.; Friesner, R. A. *J. Chem. Phys.* **2001**, *115*, 2237.
(44) Lide, D. R. *CRC handbook of chemistry and physics: a ready-reference book of chemical and physical data*, 71st ed.; CRC Press: Boca Raton, FL, 1990.
(45) Miki, N.; Maeno, M.; Maruhashi, K.; Ohmi, T. *J. Electrochem. Soc.* **1990**, *137*, 787.
(46) Wagner, W. *Properties of Water and Steam/The Industrial Standard IAPWS−IF97 for the Thermodynamic Properties and Supplementary Equations for Other Properties*; Springer−Verlag: Berlin, Germany, 1998.
(47) Keenan, J. H.; et al. *Steam Tables; Thermodynamic Properties of Water, Including Vapor, Liquid, and Solid Phases*; Wiley: New York, 1969.